Review

Toughening Mechanisms for Ceramic Materials

R. W. Steinbrech

Institute for Reactor Materials, Research Centre Jülich, Jülich, Germany

Abstract

Toughening mechanisms in ceramic materials which depend on zone and contact screening are presented and their influence on the macroscopic toughness behaviour is shown with examples.

Auf Zonen- und Kontaktabschirmung beruhende Verstärkungsmechanismen keramischer Werkstoffe wurden vorgestellt und ihre Auswirkungen auf das makroskopische Rißzähigkeitsverhalten exemplarisch demonstriert.

Nous présentons les mécanismes de renforcement des céramiques liés à l'écrantage des fissures par zones ou par contact; nous montrons, sur quelques exemples, l'influence de ces mécanismes sur le comportement de la ténacité à l'échelle macroscopique.

1 Introduction

In the last twenty years, ceramic materials have won increasing importance and significance for structural applications despite their inherent brittleness.[1,2] Progress has been prompted both by the range of applications suitable for ceramics and by the development of improved materials. In commercial practice, improved reproducibility and an associated greater reliability have been achieved as a result of systematic attention to the control of fabrication methods. In respect to materials improvements, great efforts have been and continue to be made to enhance mechanical properties through detailed microstructural design. The main objective has been to achieve an improvement in strength and a clear enhancement in toughness. Two alternative concepts for microstructural design which relate directly to the unstable behaviour of ceramic materials containing flaws, and hence determine strength and toughness, have long stood at the forefront of the developments.

Strength improvements can in the sense of the Griffith instability criterion, be achieved through a reduction in microstructural scale, provided that the critical flaw size responsible for failure correlates with the grain size. For critical flaws of approximately micrometre size, strengths of around 1 GPa are expected in a material with a toughness of 1 MPa $\sqrt{m}$. Current efforts to develop high strength monolithic fine grain ceramics provide an impressive confirmation of this fracture mechanics concept.[2,3] The strength of a ceramic can, in principle, also be increased by incorporation of a high strength second phase, provided that the stress intensity at the flaw responsible for failure is as a consequence reduced. This effect is responsible for the improved strength in the so called inclusion strengthened ceramics.[4]

The strength improvements that are won through attention to microstructural refinement and through the incorporation of load carrying inclusions are in themselves unable to reduce the extraordinary flaw sensitivity and the associated susceptibility to brittle fracture which is shown by ceramic materials. Local stress concentrations can again be responsible for catastrophic failure of the material.

An alternative concept for ceramics development has involved the search for materials which do not fail directly as a consequence of instabilities caused by existing defects but which rather show a relatively stable growth of initial flaws on loading. In contrast to the materials which have reduced flaw sizes but which nonetheless remain flaw sensitive, ceramics are now sought which can react in a tolerant way to the presence of defects either intrinsic to the material or arising from processing. Crack tolerant

behaviour becomes possible if the toughness is increased with increasing crack length (R-curve behaviour). Such an effect requires microstructural toughening mechanisms which involve increasing degrees of energy dissipation as a crack grows.

Several toughening mechanisms of this type have been developed and successfully applied in recent years to structural ceramics. They include crack deflection mechanisms, mechanisms dependent upon the development of a process zone (transformation-, microcrack-strengthening), and mechanisms dependent on crack face effects as a consequence of the presence of bridges tending to close the crack (microstructural anisotropy, incorporation of second phases).[5]

The present paper gives a brief review of strength and toughness for monolithic ceramics and then discusses the most important microstructural toughening mechanisms. The toughening influence of the latter will be considered with the help of examples from work on the crack extension of long cracks. Finally the relevance of the reported toughness behaviour for applications will be mentioned. Toughness measurements involving surface cracks will be described which show that the potential for strengthening monolithic ceramics cannot always be fully used in dealing with the failure condition.

2 Brittle Fracture

2.1 Strength and toughness

As a general rule, ceramic materials fail in a catastrophic manner after a range of elastic behaviour so that the description of this brittle

fracture behaviour can be treated with the help of linear elastic fracture mechanics. As a consequence, the two mechanical fracture parameters namely strength, σ_B, and toughness, K_{IC} can be associated with the critical crack length, a_c, by way of a crack instability criterion as proposed by Griffith.

$$\sigma_B = \frac{1}{Y} \frac{K_{IC}}{\sqrt{a_c}} \qquad (1)$$

Here Y is a parameter which is dependent on the crack and sample geometries. The equation shows directly the strength improvement which is to be expected through a reduction in the defect size, as well as indicating that changes in the toughness exert an even stronger influence on the fracture stress.

Figure 1 summarises actual strength and toughness values for commercial ceramics.[1] Strengths in the order of 1 GPa and fracture values as high as $10\,MPa\sqrt{m}$ have been reached; as expected the toughness is small in comparison to the value found for metallic materials which can be up to two orders of magnitude higher. The figure shows that a high toughness is commonly associated with a high strength. Although the experimental data points which represent mean values are widely scattered, a generally linear dependence is indicated. Formal use of eqn (1) leads, with the assumption of a surface crack of semi-circular form, to a critical crack size of approximately $a_c = 60\,\mu m$. Although such an interpretation appears reasonable, it cannot be accepted since there are a number of contradictory experimental findings.

In fine grain ceramics such as yttria stabilised zirconium oxide or silicon nitride with mean grain sizes of the order of $1\,\mu m$, none of the cracks
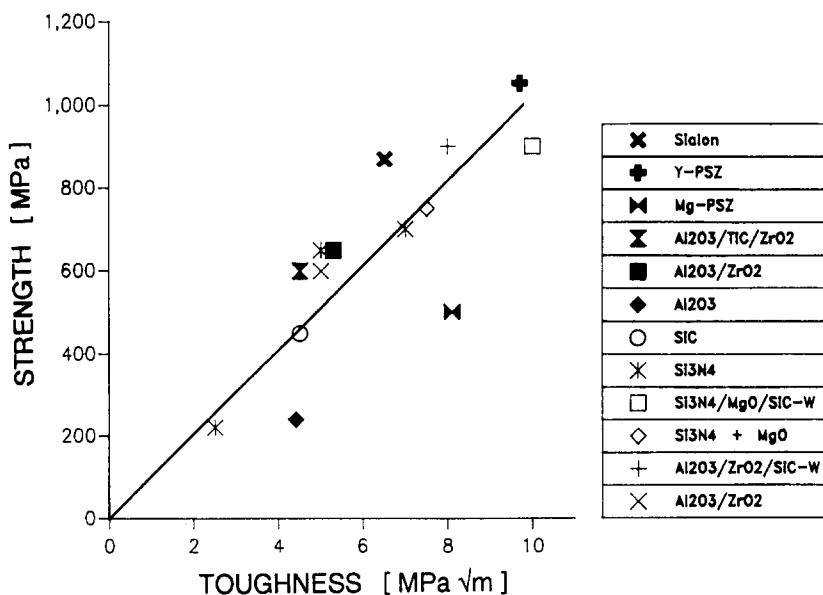

Fig. 1. Fracture data for ceramic materials. Strength and toughness results from Ref. 1.
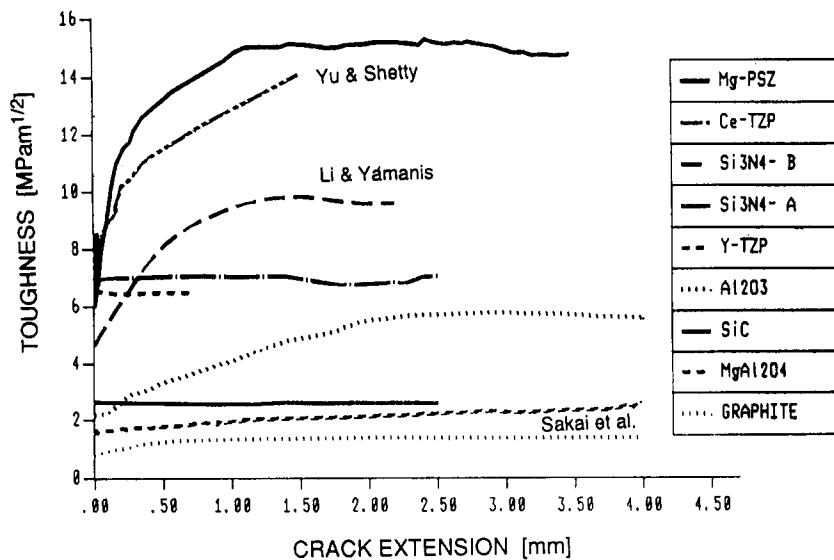
Fig. 2. *R*-curves for ceramic materials. Results of measurements on long cracks in compact tension samples. (Refs 9, 10 and 11.)

responsible for the failure of the material have been found with such dimensions. Typical values are around 10 to 20 μm.[6] In high toughness ceramics such as magnesia-partially stabilised zirconia, critical crack lengths of several hundred micrometres are in contrast found.[7] Since cracks of such a length are not *a priori* present in the ceramic but are rather developed by stable growth during loading, this means that, in terms of fracture mechanics, the toughness value itself must also have increased during loading. Equation (1) then becomes:

$$\sigma_B = \frac{1}{Y} \frac{K_R(a)}{\sqrt{a_o + \Delta a}} \qquad (2)$$

where $K_R(a)$ represents the rise in toughness with crack length (*R*-curve behaviour).

The connection between strength and toughness is, in the light of the arguments that have been made, a critical factor in the evaluation of any ceramic. This is especially true if, as a consequence of *R*-curve behaviour, maxima are observed in the $\sigma_B(K_R)$ plots as is the case for zirconia containing ceramics.[8]

2.2 *R*-curve behaviour

From research on crack extension using long cracks in standard test geometries it is known that many ceramic materials show a rise in toughness with crack length. A selection of such *R*-curves which have all been determined with compact-tension or similar test geometries is shown in Fig. 2.

Although *R*-curve behaviour is not limited to a specific toughness range, the results nonetheless show that high toughnesses in ceramics tend to result from clear *R*-curve behaviour as has been claimed by Evans.[5]

Strong *R*-curve effects showing a rising toughness on crack extensions of over 1 mm have been seen in large grain aluminium oxide,[12] in silicon nitride with high aspect ratio grains,[9] as well as in transformation toughened zirconia ceramics.[13] In contrast, flat *R*-curve behaviour is often found in fine grain ceramics such as yttria-stabilised zirconia and hot-pressed silicon nitride and silicon carbide. This does not, however, exclude *R*-curve behaviour. Rather, as has recently been often demonstrated, a steep rise in the *R*-curve at crack extensions between 10 and 20 μm occurs[6,14,15] in yttria-stabilised zirconia (YSZ) which would escape observation in experiments with CT probes. The rise which is seen in the *R*-curve and the plateau value which is found for the toughness depend on the microstructure and on the chemical composition of the ceramic as well as on the history of the crack prior to the crack extension experiment.

R-curves are also shown in Fig. 2 in the low toughness range for large grained materials (> 100 μm). It is interesting that cubic $MgAl_2O_4$ spinel[16] which, with its isotropic thermal expansion coefficient, should show no internal stresses, also shows *R*-curve behaviour. Micro-crack containing graphite also shows a rise in toughness with crack length to a small degree.[11]

3 Toughening Mechanisms

The toughening mechanisms which result in toughness enhancements in ceramic materials can be basically divided into those dependent on crack deflection and those dependent on crack screening (Fig. 3).[17]

TOUGHENING MECHANISMS

(after Ritchie, modified)

1. CRACK DEFLECTION

   AND MEANDERING

2. ZONE SHIELDING

   - TRANSFORMATION
     TOUGHENING

   - MICROCRACK
     TOUGHENING

3. CONTACT SHIELDING

   - FRICTION OF
     SERRATED GRAINS
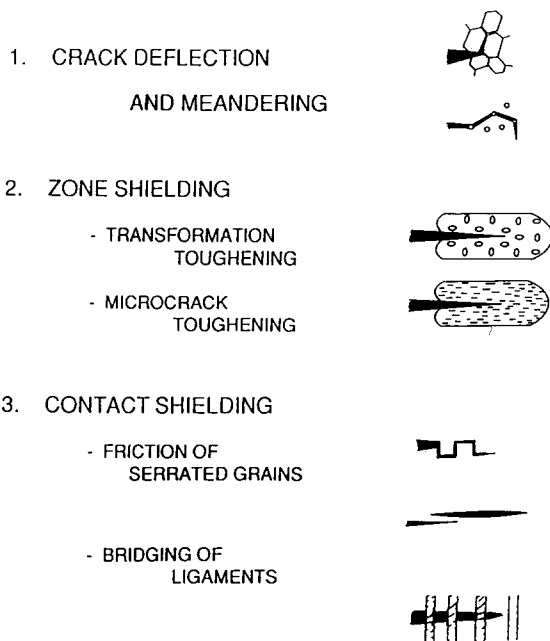
   - BRIDGING OF
     LIGAMENTS

Fig. 3. Schematic representation of the important toughening mechanisms in structural ceramics. Based on Ref. 17.

Crack deflection. Crack deflection occurs in the case of intercrystalline fracture. The effect is, for example, found in monolithic ceramics particularly in heterogenous microstructures showing anisotropic grain shape (for example needle-line grains as in silicon nitride[9]). The development of composites with localised internal stresses and with crack deflecting second phases (particles, platelets, whiskers, fibres[5]) also uses this effect. The extent of crack deflection does not in general increase with crack length so that long crack *R*-curve behaviour and a corresponding crack tolerance cannot be expected. *R*-curve behaviour requires in general toughening mechanisms which increase in effectiveness with increasing crack length.

Shielding of the crack tip. The second category of toughening mechanism arises from an increasing screening of the crack tip from the applied stress as the crack grows. This condition is automatically fulfilled if the effects which depend upon the microstructure are intensified with growing crack length. The wake-controlled *R*-curve behaviour which arises from screening effects in the region of the crack surfaces can, as has been fully described by Evans,[5] have its origins in mechanisms involving process zone screening and/or contact screening.

Zone screening occurs as a toughening effect if structural elements in a process zone surrounding the crack display hysteresis in their stress–strain

behaviour. The phase transformation in zirconia containing ceramics and stress-induced microcrack formation are examples of this toughening effect.

Contact screening has its origin in localised interactions at the crack face. Material bridges which can cause crack closing forces at the crack faces can take the form of unbroken or partially fractured grains or interlocking grains or inclusions (platelets, whiskers, fibres, metallic phases); these bridge the crack and hinder crack opening. For a separation of the crack surfaces, additional energy is needed which then appears in macroscopic terms as an increased toughness.

It should be emphasised that a clean separation of the several screening effects is not always possible and, indeed, is not always present. It can happen that zone-screening and contact screening arise simultaneously and synergetic effects then produce a higher resulting toughness than would be expected for the individual mechanisms.

The micro-mechanics modelling of screening effects in the context of the macroscopic toughness is generally developed on the basis of energy concepts.[4,5] An energy term which arises from the screening effect is then added to the local energy requirement for the occurrence of fracture at the crack tip (G_0).

$$K_R = [E(G_0 + \Delta G_c)]^{1/2} \tag{3}$$

The toughness and energy requirement have been linked in eqn (3) in the usual manner by way of the modulus of elasticity (E).

In the case of process zone toughening (Fig. 4, upper diagram), the contribution to ΔG_c arises from the irreversible deformation behaviour of the individual toughening elements during the passing of the local stress field of the crack. The hysteresis in the stress–strain behaviour (transformations, microcrack formation, etc.) represents additional energy dissipation. The required energy is dependent on the size of the process zone (h) as well as on the density of the active non-linear elements (f_z).

$$\Delta G_c = 2f_z\sigma_0\cdot\varepsilon_0\cdot h \tag{4}$$

For a given degree of hysteresis, the parameters of interest for materials development are in particular f_z and h.

In the case of contact screening by way of bridges between the crack faces, the energy dissipation arising from the separation of the interacting elements (Fig. 4, lower diagram) is responsible for the additional toughening effect.

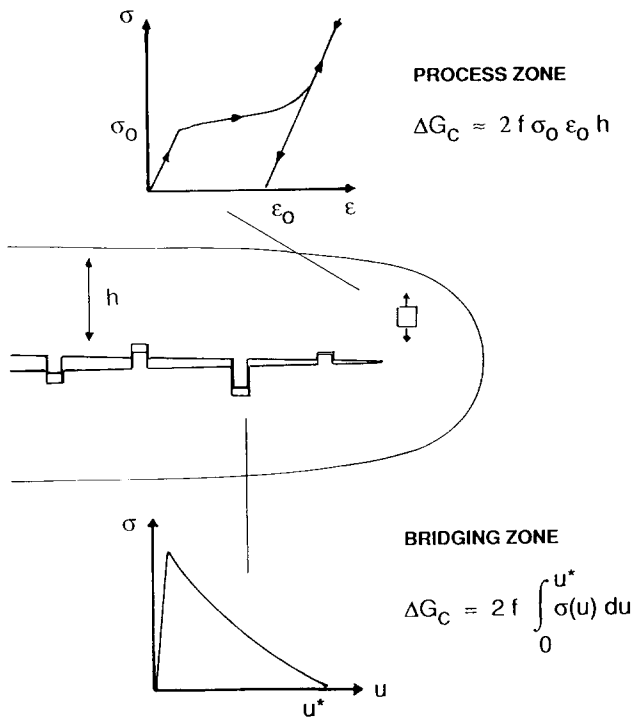$$\Delta G_c = 2f_B \int_0^{u_{max}} \sigma(u)\,du \tag{5}$$

Fig. 4. Toughening of ceramics by zone- and contact-screening. Energy dissipation in the corresponding toughening elements is indicated.

For a given bridging element, the maximum separation distance, u_{max}, is determined by the point at which the crack closing force goes to zero in the stress versus crack opening distance behaviour. The density of active crack bridges is taken care of in the parameter f_B. In seeking a successful toughening for the material through crack face bridges, it is important to consider all those microstructural elements which lead to a greater area under the stress versus crack face separation curve. An extreme example in this connection is given by the friction controlled pull out behaviour found in fibre strengthened composites.[18]

Following this survey of toughening mechanisms which arise through crack screening, results are given from studies of crack extension behaviour which should help to clarify further the basic features of this mode of toughening for ceramic materials.

3.1 Zone screening

3.1.1 Transformation toughening

The effectiveness of transformation toughening in zirconia-containing ceramics is shown especially clearly by the example of magnesia–partially stabilised zirconia (Mg–PSZ). Striking R-curve behaviour with a plateau toughness of around 18 MPa $\sqrt{m}$ can be achieved by optimisation of the stress-induced microstructural transformations that are found in certain materials groups.[13]

In Mg–PSZ, metastable tetragonal (t) precipitates form the strengthening elements in the process zone. In the stress field of the crack, there occurs a volume dilatation and a shearing as the elements transform to the equilibrium monoclinic (m) symmetry. The size of the transformation zone which surrounds the crack is dependent on the transformation behaviour of the t-precipitates; the toughening effect is also determined by the number density of the transforming precipitates.

In high toughness Mg–PSZ, transformation zones of up to 1 mm (h) can be formed.[19] As a consequence of the volume dilatation during the tetragonal to monoclinic transformation ($\Delta V = 4 \cdot 7\%$ in the absence of constraints[20]), the zone can be optically observed[21] in the form of surface uplifting. Although there is currently no exact correlation between microstructure, zone size and R-curve behaviour,[5] it has long been recognised that selected heat treatments can be used to influence the transformation tendency of the tetragonal precipitates and hence the transformation toughening of the material.[22]

Crack extension curves are consistent with the macroscopic changes in toughness behaviour. Results for a 9·7 mol.% Mg–PSZ are shown in Figs 5 and 6. Following a dissolution treatment at 1700°C and a quick quench, the material is held at 1400°C for up to a maximum of 10 h. Some samples undergo an additional heat treatment at 1100°C with different isothermal holds of up to 2 h. Figure 5 shows the change in the size of precipitates which results from the 1400°C heat treatment. The subeutectoid anneal at 1100°C produces no further growth in the precipitates but results in the formation of a magnesia rich $Mg_2Zr_5O_{12}$ (δ) phase around them which acts favourably on the transformation.[23]

The R-curves in Fig. 6 are found in compact-tension samples following the annealing treatment; they reveal significant differences following a certain crack extension. For the Mg–PSZ material under study, an optimal toughening effect is found in a heat treatment of 2 h at 1400°C followed by one of 1·5 h at 1100°C. The toughness rises from a value of 4 MPa $\sqrt{m}$ in the material without precipitates to a value 12 MPa $\sqrt{m}$ at the plateau following an optimisation of the transformation conditions.
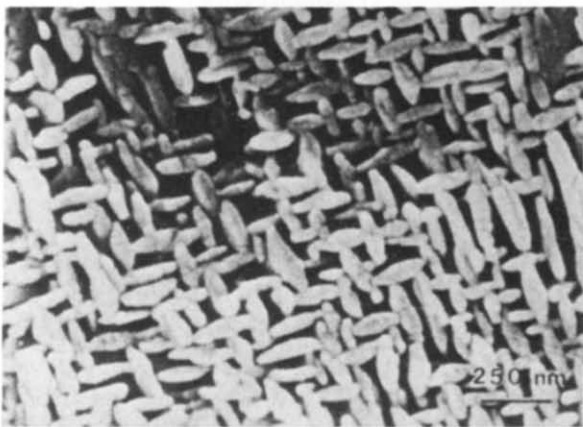
3.1.2. Microcrack toughening

Analogous to the t–m transformation behaviour of zirconia, stress-induced microcrack formation represents an irreversible deformation phenomenon which is associated with energy dissipation and which consequently makes a contribution to a rise in
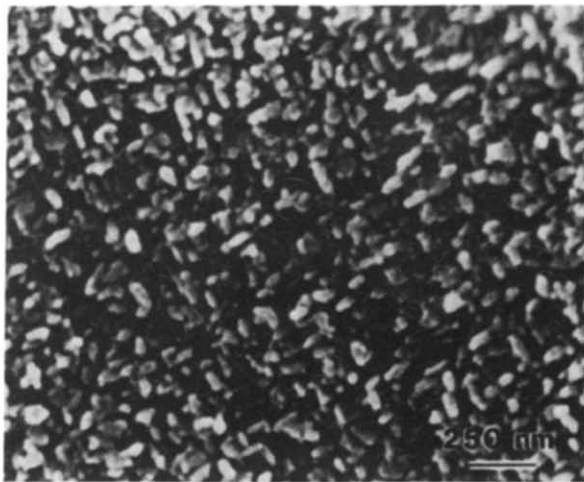
(a)
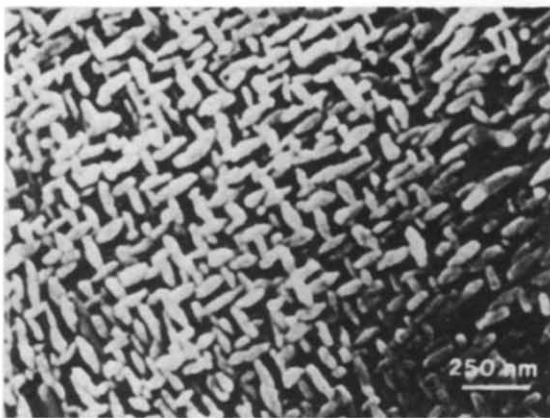
(b)

(c)

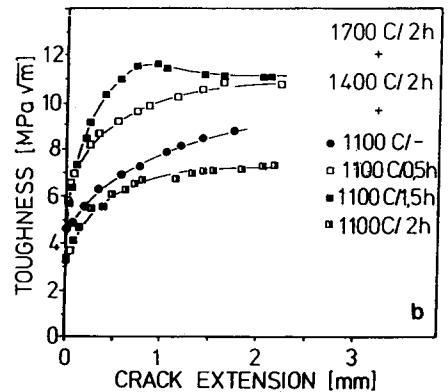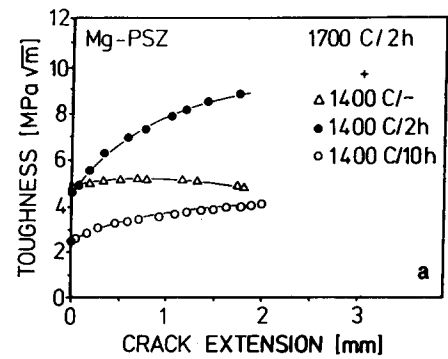**Fig. 5.** Aging of Mg–PSZ precipitates. (a) Solution heat treatment. (b) 1400°C, 2 h. (c) 1400°C, 10 h.

Fig. 6. Influence of heat treatment on the *R*-curve behaviour of Mg–PSZ. (a) For the microstructures in Fig. 5. (b) Following additional subeutectoid annealing at 1100°C.

toughness.[5,24] Confirmation of microcrack toughening has been recently found for a silicon carbide–titanium diboride composite ceramic which has shown *R*-curve behaviour; the microcracking in a process zone around the main crack could be observed both directly with the transmission electron microscope and indirectly with the help of small angle X-ray spectroscopy (SAXS).[25]

For the toughening of the silicon carbide ceramics, TiB_2 particles are incorporated, which have a higher thermal expansion coefficient ($\alpha_{SiC} = 5\cdot6\cdot10^{-6}/K$, $\alpha_{TiB2} = 8\cdot5\cdot10^{-6}/K$). Crack extension experiments with compact tension samples demonstrated by way of scanning optical microscopy effects predominantly associated with crack deflection and interlocking (Fig. 7). However, it is clear from the mechanical compliance behaviour as well as from
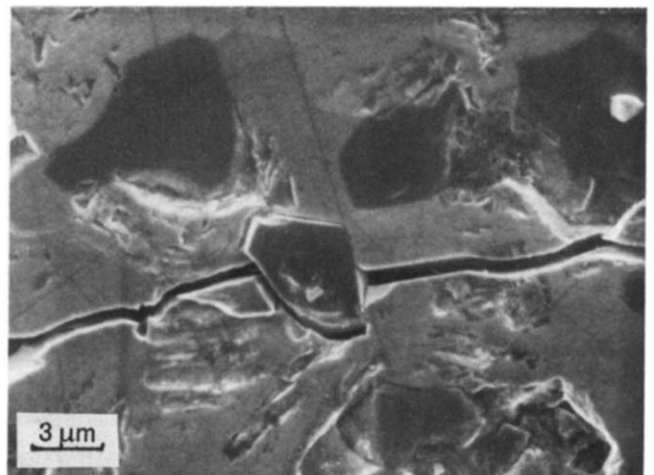

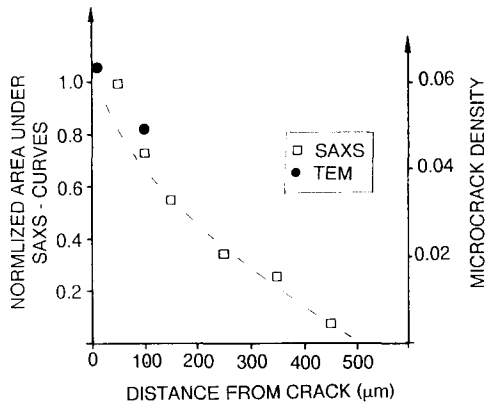**Fig. 7.** Crack path in $SiC–TiB_2$ composite ceramics. The incorporated TiB_2 grains show dark contrast.

Fig. 8. Microcrack process zones in SiC–TiB$_2$. Density of microcracks as observed in TEM and SAXS.
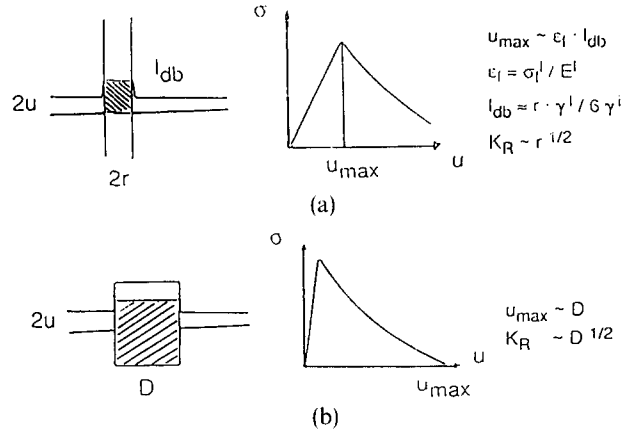

Fig. 9. Toughening through bridges between the crack faces. (a) Energy dissipation by elastic deformation of the bridges. (b) Energy dissipation by friction controlled separation of the crack faces.

the microstructural studies, that zone screening as a consequence of microcrack formation is dominant. The dependence of the microcrack density on the distance from the crack (x) gives consistent results both for TEM and for SAXS (Fig. 8). The microcrack density falls with increasing distance from the crack; zone sizes have a maximum value of 400 to 500 μm (h). With TiB$_2$ particles and microcrack formation, the toughness is virtually doubled from $K_R = 3\,\text{MPa}\sqrt{m}$ for silicon carbide to $K_R = 6 \cdot 5\,\text{MPa}\sqrt{m}$ as the plateau value of the R-curve for a SiC–23·3 vol.% TiB$_2$ material.[25]

3.2 Contact screening

The screening of the crack tip from the imposed stress as a consequence of crack face contacts was first found in large grain aluminium oxide ceramics.[26] Several elastic and inelastic crack bridging forms have since been observed in ceramic materials.[27]

In the stress-separation behaviour of crack face bridges which provide a crack closing force, it is possible to distinguish between two toughening contributions (Fig. 9); these can be more fully explained in idealised form.

For the most part, only the elastic extensions of the bridging element influences the crack opening behaviour; after a maximum stress value, σ_{max} (u), has been reached, rapid failure results (Fig. 9(a)). The maximum extension (u_{max}) depends in this case on the elastic strain (ε_f) as well as on the debonding length (l_{db}) of the bridging element that has been freed from the surrounding microstructure.

$$u_{max} = \varepsilon_f \cdot l_{db} \qquad (6)$$

where[28] ε_f is equal to σ_f^l/E^l and[28] $l_{db} = r \cdot \gamma^l/6\gamma^i$.

Here σ_f^l represents the fracture stress, E^l represents the elastic modulus, γ^l represents the work of fracture and r the radius of the bridging element; γ^i is

the work of fracture at the interface with the matrix. Large elastic extensions then result from weak interfaces and high strength and toughness in the bridging materials. The interface properties have in particular been considered in a number of the contributions to the present volume. According to Becher,[4] consideration of the elastic separation behaviour leads to the conclusion that the toughness can be enhanced by bridging elements of large radius according to $K_R = K_R(r^{1/2})$.

In the case of intercrystalline fracture with interlocking crack surface grains, the frictional behaviour plays the main role in determining the additional energy of separation. In this case, the significant contribution is made by the falling region in the $\sigma(u)$ curve (Fig. 9(b)). The maximum separation distance at which a closing force remains active can then be correlated with the grain size (D).

$$u_{max} = D \qquad (7)$$

Assuming equiaxed grains, the toughness again depends on the average grain size according to the relation $K_R = K_R\ (D^{1/2})$.

For both toughening mechanisms, namely elastic bridges and frictional contacts, material examples can be usefully considered.

3.2.1 Crack face interactions in Si_3N_4

A most promising direction for materials development lies in the strengthening of silicon nitride by way of in-situ growth of high aspect ratio grains during the sintering stage.[4,9] Toughness values of greater than 10 MPa $\sqrt{m}$ have been reported; the crack extension experiments of Li and Yamanis[9] also indicate that this value represents the plateau of a pronounced R-curve behaviour. The toughening effect can be attributed to crack bridges which are formed by the whisker-like grains. With suitable
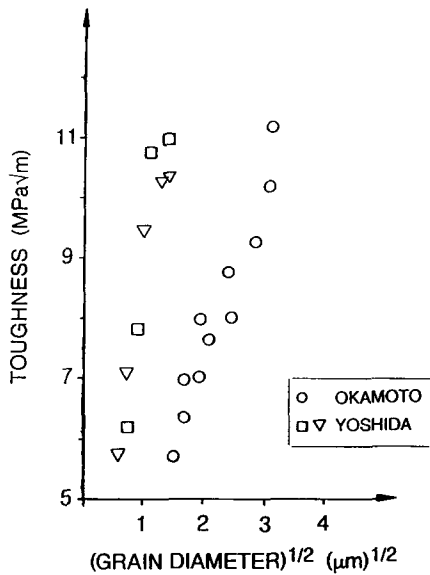
Fig. 10. Toughness of in situ strengthened Si_3N_4 ceramics as a function of the diameter of the elongated grains. Refs 29 and 30.)

Fig. 11. Interactions at the crack faces in large grained Al_2O_3.

choice of the sintering conditions (temperature, heating time), it is possible to control the diameter and the length of the grains. The dependence of the toughness on such microstructural changes is shown in Fig. 10 where the results of several authors[29,30] are summarised. It is seen that the relation proposed by Becher[4] where K_R is proportional to $\sqrt{D}$ is clearly supported by the experimental results.

3.2.2 Crack face interactions in Al_2O_3

Al_2O_3 is the ceramic material which has been most studied[26,31-33] in connection with R-curve behaviour arising from contact screening. Using re-notch experiments (removal of the crack faces following a given crack growth) attention has been given to the toughening mechanisms which arise behind the crack tip (wake-effects).[26] Crack face interactions arise from the change in crack path development which occurs in large grained alumina ceramics at increased crack opening (Fig. 11). The freeing of local keying points by the forming of side cracks can be seen in the two light micrographs which show the samples after two stages of crack growth. The crack face contacts exerting closing forces are not limited to the sample surface but occur also in the bulk of the material. Figure 12 indicates qualitatively this effect in a two-step crack extension experiment with large-grained alumina ($D = 20\,\mu m$). In crack extension experiments using short double cantilever beam samples, stable cracks of a given length can be enlarged (Fig. 12(a)). From the force displacement behaviour—with the characteristic departure from the linear elastic rise before reaching the maximum and with the following gradual
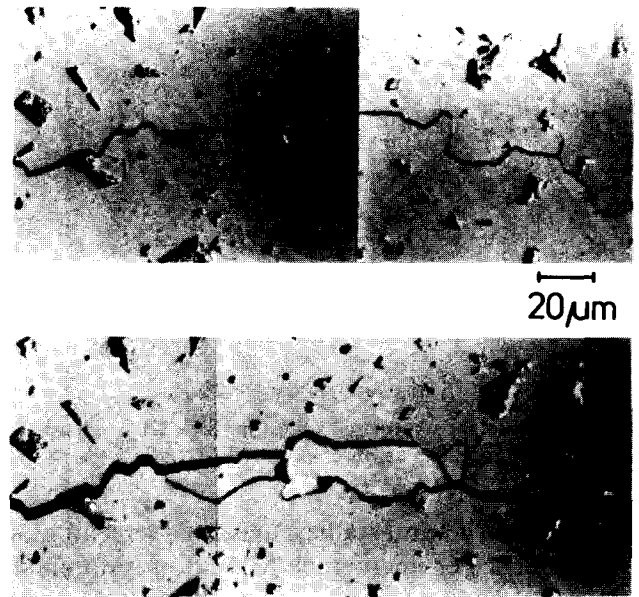
reduction in required load—it is clear that the alumina ceramic demonstrates R-curve behaviour. In the second part of the experiment, a tensile load is applied to the sample after a counter-notch has been made up to the crack tip (Fig. 12(b)). It is then clear that the material which has already been broken can only be fully separated with further energy dissipation owing to interlocking material at the crack
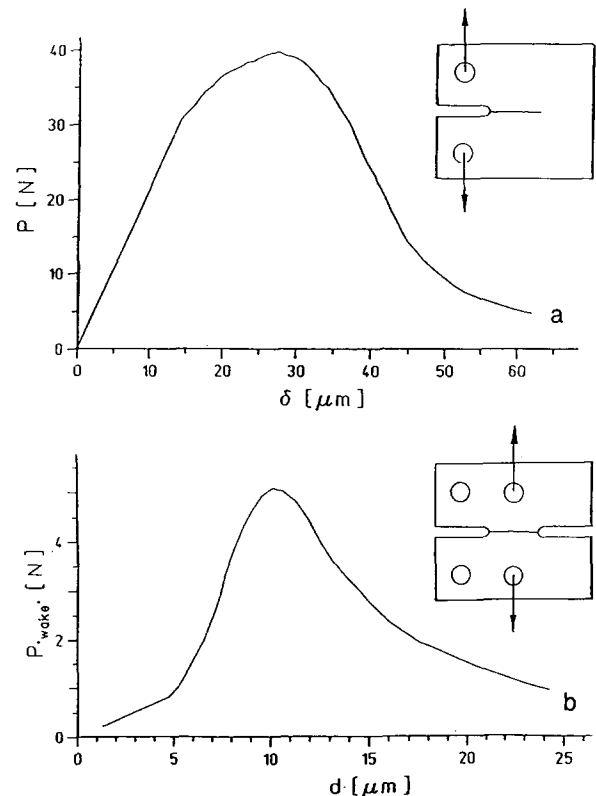

Fig. 12. Indication of energy dissipation during crack face separation. (a) CT crack extension experiment with defined crack lengthening. (b) Tensile loading of the crack face region following the removal of the unbroken section of the sample.

faces. Systematic measurements with a similar method made by White *et al.*[34] confirm the existence of this toughening mechanism for a variety of oxide materials.[34]

Micromechanic modelling of the interlocking effect for the friction control separation of the bridging elements leads to[35]

$$\sigma(u) = \sigma_m\left(1 - \frac{u}{u_{max}}\right)^n \tag{8}$$

where the stress falls from a maximum value $\sigma = \sigma_m$ directly behind the crack tip (crack opening $u = 0$) to the value $\sigma = 0$ at the end of the crack face interaction zone (where $u = u_{max}$) at a rate dependent upon the parameter n.

For the modelling of toughness from long cracks in test geometries of limited sample size, eqn (5) is changed to[33]

$$\Delta G_c = 2\int_0^{z_{max}} \sigma u(z)\frac{du}{da}\,dz \tag{9}$$

where z is taken parallel to the crack.

Equation (9) contains a geometry dependence of the toughening effect which can be derived[36] on the basis of the methods of weight functions and which has also been found experimentally[31] from measurements with different crack and test geometries. The grain size dependence of the R-curve behaviour of Al_2O_3 (Fig. 13) is likewise explained by the toughening model of crack face bridges when reference is made[26] to the respective maximum separation length $u_{max} \propto D$.

3.3 Potential for toughening

The currently achieved potential for toughening in ceramic materials is quoted as $K_R = 10\,MPa\sqrt{m}$ for
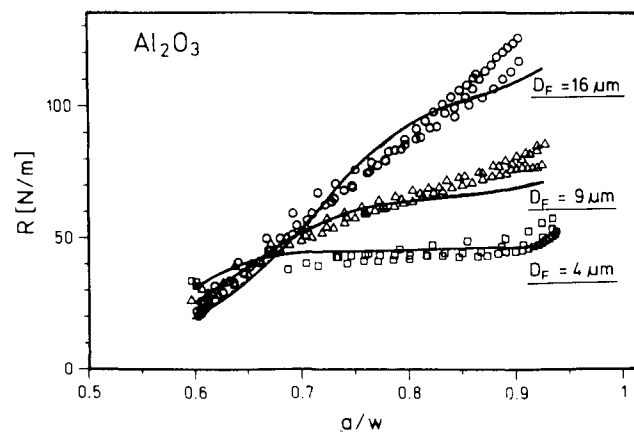

Fig. 13. Influence of grain-size on the R-curve behaviour of Al_2O_3 ($R = K_R^2/E$). The crack face model (indicated curves) is in good agreement with the measured values.

microcrack formation, $K_R = 20\,MPa\sqrt{m}$ for zirconia transformations and $K_R = 10$ to $15\,MPa\sqrt{m}$ for the use of brittle inclusions.[5] In the context of R-curve behaviour, such figures correspond to the plateau value of long cracks; this is often reached only after pronounced crack extension. The question of whether these material improvements which are considerable for a ceramic can be really used under the failure conditions set by applications must finally be settled by toughness measurements on 'naturally' occurring surface cracks.

4 Toughness Behaviour for Surface Cracks

The studies of crack extension which are relevant for component failure should be based on the extension and toughness behaviour of natural defects and of short cracks. The R-curve behaviour of short cracks —often initiated by hardness indents—has been extensively studied by Lawn and co-workers.[32,35] The results for alumina ceramics are in qualitative agreement with observations on long cracks, i.e. crack bridging effects represent the significant toughening mechanisms. However, to characterise the initial toughness behaviour of ceramic materials on the basis of such studies, it is necessary to make crack extension measurements on the same 'naturally' occurring cracks which determine the strength. In experimental terms, this means that the extension of 'natural' cracks must be observed in-situ. For ceramics with R-curve behaviour, this requirement is for a limited degree of crack growth satisfied. It can be shown with an energy balance that stable crack growth occurs over a limited range in the case of R-curve behaviour.[37] Up to present, however, relatively few measurements of this kind are known.[7,38-41]

Crack extension measurements using 'naturally' occurring cracks can be made in bend tests. The sample is loaded in a stepwise manner and the tension face is scanned microscopically in situ to observe crack formation and growth. The toughness is then given directly from eqn (1) on the basis of the crack depth profile of the crack that is formed and on the basis of the imposed edge fibre tensile stress. The loading of the sample occurs stepwise with controlled bending in order to simplify the task of tracing the crack.

Figure 14 shows a light microscope photograph of a 'naturally' occurring surface crack in large grain Al_2O_3; crack growth is shown for different loading steps. The resulting R-curve behaviour of the surface cracks is shown in Fig. 15 together with the
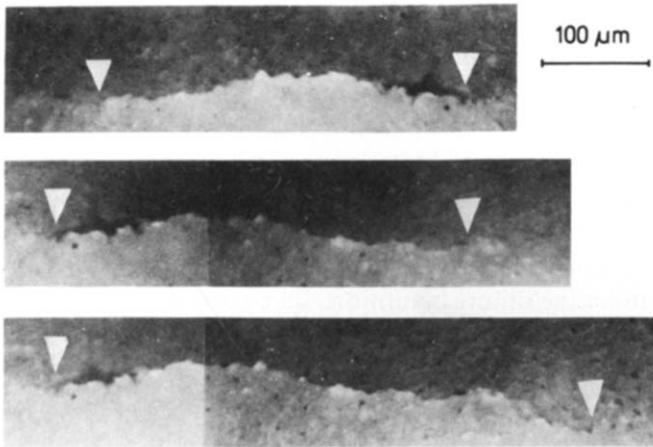
Fig. 14. Growth of natural surface cracks in large grained Al_2O_3. Light micrographs of the tensile surface of a bend sample.

Fig. 16. 'Natural' surface crack in high toughness MG-PSZ.

corresponding R-curves for indent cracks and long cracks arising from SENB bend test samples. The R-curves of the short cracks begin at a significantly smaller stress intensity. Crack instability occurs clearly before the plateau toughness of long cracks is reached. The low toughness at the point of crack initiation for naturally occurring surface cracks arises most probably from localised microstructural inhomogeneities. These either contribute to a weakening of the material or are responsible for internal stress fields.[42] The formation of more than one crack is often observed. All of the cracks can grow during the loading but the one with the flattest R-curve rise will be the first to become unstable; it determines the strength of the ceramic.

Similar R-curve results have been found with short cracks in Mg-PSZ (Figs 16 and 17). Crack initiation again arises at very small stress intensities and the high plateau value for the toughness is again
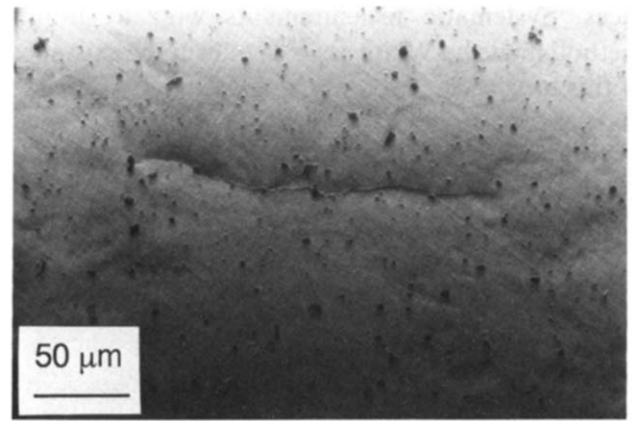
not reached since the naturally occurring surface cracks become unstable.

The differences in toughness behaviour between 'natural' and long cracks are important for applications. Under the conditions of failure that are technically relevant and which correspond to the damage arising from 'natural' surface cracks, ceramic pieces are clearly unable to reach the full potential of the R-curve behaviour for the material. Toughness data given on the basis of plateau values for long cracks overestimate, particularly in the case of striking R-curve behaviour, the properties of the material. It must also be noted that stable growth of 'natural' cracks is often not to be found in standard loading situations. Since the influence of short cracks on the compliance of the component is small, ceramics behave as linear elastic materials despite the R-curve behaviour.

Even the connections which have been described in Section 2.1 between the strength and toughness require a re-evaluation in the light of the crack
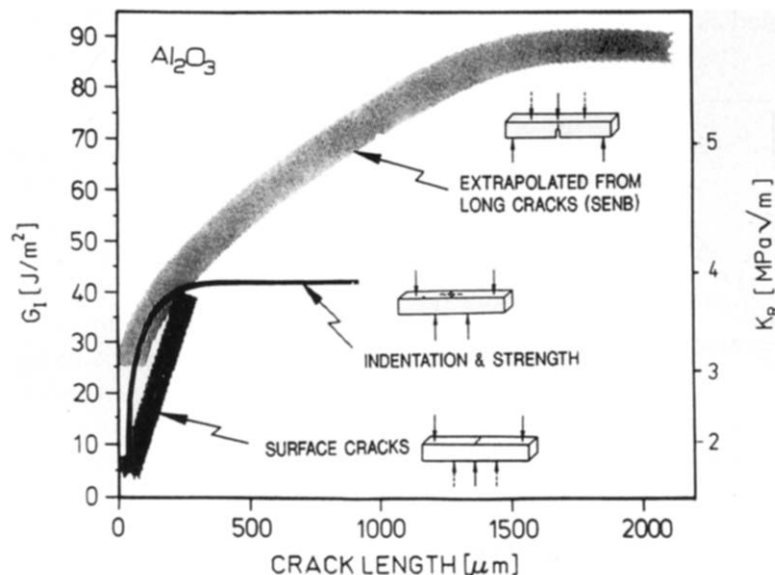

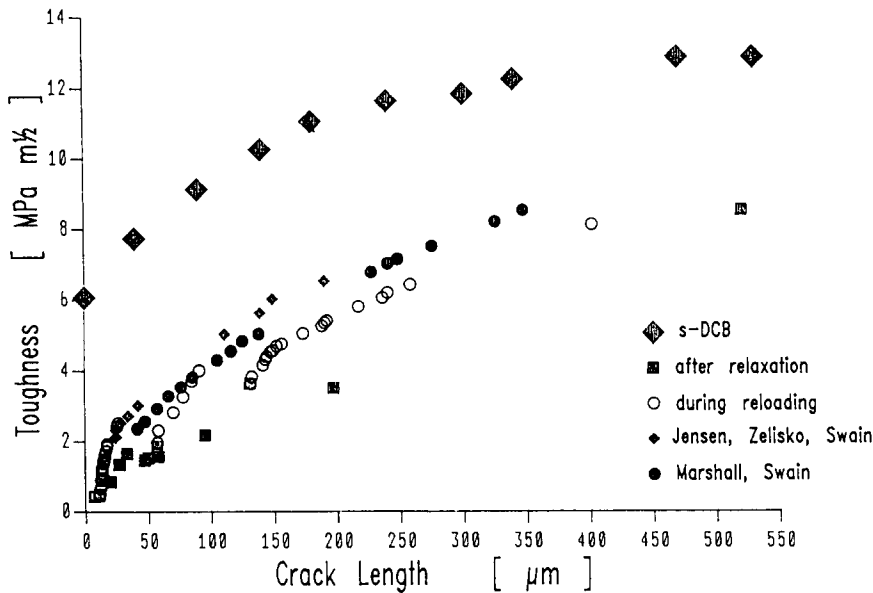Fig. 15. Comparison of toughness development for 'natural', hardness indent and long cracks (SENB) in Al_2O_3.

Fig. 17. Comparison of the toughness behaviour of 'natural' and long cracks in Mg–PSZ. (Refs 39 and 40).

extension behaviour of 'natural' surface cracks. A correlation is only meaningful if both fracture parameters are reported for the same crack geometry. Since crack instability does not occur in the plateau region, the concentration at the maximal toughness as measured in long crack experiments is of little help for performance criteria. With reference to toughening mechanisms, it is much more important to optimise the R-curve rise, so that a certain crack tolerance occurs alongside a high strength. Such a result can be demonstrated successfully with Mg–PSZ where a bend test strength of $\sigma_B = 600$ MPa and a toughness of $K_R = 8 \cdot 5$ MPa $\sqrt{m}$ can result after stable growth of natural cracks to the extent of $\Delta a = 160 \, \mu m$. A more crack tolerant version with $\sigma_B = 400$ MPa and $K_R = 8 \cdot 5$ MPa $\sqrt{m}$ allows stable crack extension for as much as $\Delta a = 350 \, \mu m$.[39]

5 Conclusions

Toughening mechanisms in ceramic materials which depend on zone and contact screening are presented and their influence on the macroscopic toughness behaviour is shown with examples.

The conclusion is that especially for the case of long range toughening effects, the full potential for toughening cannot be exploited under conditions that are relevant for applications.

Materials development should, therefore, be directed in the case of crack tolerant ceramics with R-curve behaviour, to an optimisation of the R-curve rise targetted on strength, toughness and stable crack extension.

References

1. Willmann, G. & Wielage, B. (Hrsg.), *Technische Keramik.* Vulkanverlag, Essen, 1988.
2. *New Technology in Japan, Hyper-Reliable Integrated Materials R&D in Japan.* Special issue, Jetro, Three 'I' Publications, Tokyo, 1991.
3. Niihara, K., *New Design of Structural Ceramics-Nanocomposites*, *Proc. ECERS 2*, Augsburg, 1991. Deutsche Keramische Gesellschaft (in press).
4. Becher, P. F., Microstructural design of toughened ceramics. *J. Am. Ceram. Soc.*, **74** (1991) 255–69.
5. Evans, A. G., Perspective of the development of high toughness ceramics. *J. Am. Ceram. Soc.*, **73** (1990) 187–206.
6. Anderson, R. M. & Braun, L. M., Technique for R-curve determination of Y-TZP using indentation produced flaws. *J. Am. Soc.*, **73** (1990) 3059–62.
7. Dransmann, G. & Steinbrech, R. W., Toughness of surface cracks in MgO partially stabilized zirconia. *Fortschrittsberichte DKG*, **5** (1990) 53–67 (in German).
8. Swain, M. V., Inelastic deformation of Mg–PSZ and its significance for strength toughness relationships of zirconia toughened ceramics. *Acta Metall.*, **33** (1985) 2083–91.
9. Li, Ch-Wei & Yamanis, J., Super-tough silicon nitride with R-curve behavior. *Ceram. Eng. and Sci. Proc.*, **10**, 7–8 (1989) 632–45.

10. Yu, C.-S. & Shetty, D. K., Transformation zone shape, size and crack growth resistance (R-curve) of ceria partially stabilized zirconia polycrystals. J. Am. Ceram. Soc., 72 (1989) 921–8.

11. Sakai, M., Yoshimura, J. L., Goto, Y. & Inagaki, M., R-curve behavior of a polycrystalline graphite: microcracking and grain bridging in the wake region. J. Am. Ceram. Soc., 71 (1988) 609–16.

12. Steinbrech, R. W., Knehans, R. & Schaarwächter, W., Increase of crack resistance during slow crack growth in Al₂O₃ bend specimens. J. Mater. Sci., 18 (1983) 265–70.

13. Heuer, A. H., Readey, M. J. & Steinbrech, R. W., Resistance curve behavior of supertough MgO partially stabilized zirconia. Mat. Sci. Engng. A, 105/106 (1988) 83–89.

14. Liu, S.-Y. & Chen, I. W., Fatigue of yttria-stabilized zirconia: II, crack propagation, fatigue striations, and short-crack behavior. J. Am. Ceram. Soc., 74 (1991) 1206–16.

15. Pajares, A., Guiberteau, F., Dominguez, A., Dransmann, G. & Steinbrech, R. W., Propagation of short surface cracks in Y–TZP. Proc. ECERS 2, Augsburg, 1991. Deutsche Keramische Gesellschaft (in press).

16. Readey, M. J. & Steinbrech, R. W., R-curve behavior in transparent MgAl₂O₄ spinel ceramics. Annual Meeting Am. Ceram. Soc., Cincinnati, OH, 1991 (in press).

17. Ritchie, R. O., Mechanisms of fatigue crack propagation in metals, ceramics and composites; role of crack tip shielding. Mat. Sci. Engng., A103 (1988) 15–28.

18. Fuller, E. R., Butler, E. P. & Carter, W. C., Determination of fiber-matrix interfacial properties of importance to ceramic composite toughening. Proceedings, Nato Advanced Research Workshop: Toughening Mechanisms in Quasi-Brittle Materials, ed. P. Shah. NATO ASI Series E, Vol. 195, Kluwer Academic, Publishers, Dordrecht, 1991, pp. 385–404.

19. Dauskardt, R. H., Veis, D. K. & Ritchie, R. O., Spatially resolved Raman spectroscopy of transformed zones in magnesia partially stabilized zirconia. J. Am. Ceram. Soc., 72 (1989) 1124–9.

20. Rühle, M. & Heuer, A. H., Phase transformations in ZrO₂-containing ceramics: II, the Martensitic reaction in t-ZrO₂. In Science and Technology of Zirconia II, Advances in Ceramics, Vol. 12, ed. N. Claussen, M. Rühle & A. H. Heuer. Am. Ceram. Soc., Columbus, OH, 1984.

21. Steinbrech, R. W., Inghels, E. & Heuer, A. H., Residual displacement effects during crack propagation in high-toughness magnesia-partially stabilized zirconia. J. Am. Ceram. Soc., 73 (1990) 2016–22.

22. Swain, M. V. & Hannik, R. H. J., R-curve behavior of zirconia ceramics. In Science and Technology of Zirconia II, Advances in Ceramics, Vol. 12, ed. N. Claussen, M. Rühle & A. H. Heuer. Am. Ceram. Soc., Columbus, OH, 1984.

23. Green, D. J., Hannik, R. H. J. & Swain, M. V., Transformation Toughening of Ceramics. CRC Press, Boca Raton, 1989.

24. Buresch, F. E., A structure sensitive K_{IC}-value and its dependence on grain size distribution, density and micro-crack interaction. In Fracture Mechanics of Ceramics, Vol. 4, ed. R. C. Bradt, D. P. H. Hasselman & F. F. Lange. Plenum, New York, 1975, pp. 835–47.

25. Gu, W. H., Faber, K. T. & Steinbrech, R. W., Microcracking and R-curve behavior in SiC–TiB₂. Acta Met. (in press).

26. Knehans, R. & Steinbrech, R. W., Memory effect of crack resistance during slow crack growth in notched Al₂O₃ bend specimens. J. Mat. Sci. Letters, 1 (1982) 327–9.

27. Rödel, J., Interaction between crack deflection and crack bridging. J. Eur. Ceram. Soc. (this issue), 10 (1992) 143–50.

28. Budianski, B., Hutchinson, J. W. & Evans, A. G., Matrix fracture in fiber-reinforced ceramics. J. Mech. Phys. Solids, 34 (1986) 167–89.

29. Okamoto, H. & Kawashima, T., as stated in Ref. 4.

30. Yoshida, A., Development of High Toughness Silicon Nitride Ceramics. Denki Kagaku Kogyo Co., Japan (in press).

31. Steinbrech, R. W., Reichl, A. & Schaarwächter, W., R-curve behavior of long cracks in alumina. J. Am. Ceram. Soc., 73 (1990) 2009–15.

32. Bennison, S. J. & Lawn, B. R., Flaw tolerance in ceramics with rising crack resistance characteristics. J. Mater. Sci., 24 (1989) 3169–75.

33. Nickel, H. & Steinbrech, R. W. (ed.), Microfracture in Al₂O₃ ceramics. Proceedings of a Research Project of the German Research Association (DFG). Research Center Jülich, 1991 (in German).

34. White, K. W. & Kelka, G. P., Evaluation of the crack face bridging mechanisms of MgAl₂O₄ spinel. JACS (submitted).

35. Mai, Y. W. & Lawn, B. R., Crack interface grain bridging as a fracture resistance mechanism in ceramics: II, a model. J. Am. Ceram. Soc., 70 (1987) 289–94.

36. Fett, T. & Munz, D., Influence of crack surface interactions on stress intensity factor in ceramics. J. Mat. Sci. Letters, 9 (1990) 1403–6.

37. Atkins, A. G. & Mai, Y.-W., Elastic and Plastic Fracture: Metals, Polymers, Ceramics, Composites, Biological Materials. Ellis Harwood Ltd., Chichester, UK, 1985.

38. Marshall, D. B., Strength characteristics of transformation toughened zirconia. J. Am. Ceram. Soc., 69 (1986) 173–80.

39. Steinbrech, R. W. & Schmenkel, O., Crack resistance curves of surface cracks in alumina. J. Am. Ceram. Soc., 71 (1988) 271–3.

40. Marshall, D. B. & Swain, M. V., Crack resistance curves in magnesia partially stabilized zirconia. J. Am. Ceram. Soc., 71 (1988) 399–407.

41. Jensen, D. B., Zelizko, V. & Swain, M. V., Small flaw static fatigue crack growth in Mg–PSZ. J. Mat. Sci. Letters, 8 (1989) 1154–7.

42. Fett, T. & Munz, D., Why can microcracks in ceramics propagate at extremely low stress intensity factors? J. Mat. Sci. Lett., 11 (1992) 257–60.